Journal of Electrostatics 72 (2014) 462–469

Contents lists available at ScienceDirect

Journal of Electrostatics

journal homepage: www.elsevier.com/locate/elstat

Electrospun precursor carbon nanofibers optimization by using response surface methodology

Ashraf A. Ali [a, *], M.M. Eltabey [b], W.M. Farouk [c], Said H. Zoalfakar [d]

[a] Mechanical Design and Production Engineering Department, Faculty of Engineering, Zagazig University, P.O. Box 44519, Egypt
[b] Basic Engineering Science Department, Faculty of Engineering, Menoufiya University, Egypt
[c] Mechanical Engineering Department, Faculty of Engineering, Banha University, Egypt
[d] Mechanical Engineering Department, The Higher Technological Institute (HTI), Egypt

ARTICLE INFO

Article history:
Received 21 February 2013
Received in revised form
27 June 2014
Accepted 15 September 2014
Available online 27 September 2014

Keywords:
Electrospinning
Carbon fiber
Microstructures
Statistical properties method
Scanning electron microscopy

ABSTRACT

Ultrafine fibers were electrospun from Polyacrylonitrile and N,N-dimethylformamide solution to be used as a precursor for carbon nanofibers. An electrospinning set-up was used to collect fibers with diameter ranging from 104 nm to 434 nm. Morphology of fibers and its distribution were investigated by varying Berry's number, charge density, spinning angle, spinneret diameter and collector area. A more systematic understanding of process parameters was obtained and a quantitative relationship between electrospinning parameters and average fiber diameter was established by using response surface methodology. It was concluded that; Berry's number, charge density and spinneret diameters played an important role to the diameter of nanofibers and its standard deviation. Spinning angle and collector area had no significant impact. Based on response surface methodology the optimum Polyacrylonitrile average fiber diameter of 280 nm and 28 nm standard deviation, were collected at 1.6 kV/cm charge density, 8 Berry's number and 0.9 mm spinneret diameter.

Introduction

The electrospinning technology has been known for a long time. Zeleny [1] presented one of the earliest studies of the electrified jetting phenomenon; the role of the surface instability in electrical discharges from charged droplets has been studied in this paper.

Between 1934 and 1944, Formhals [2–5] published a series of patents describing an experimental setup for the production of polymer filaments using electrostatic forces. In 1966, Simons [6] patented an apparatus for the production of patterned, ultrathin, low weight, non-woven fabrics using electrical spinning.

Taylor [7–10] studied the stable shape of charged liquid drops that was deformed by an electric field into a conical geometry now known as a Taylor cone.

In 1971, Baumgarten [11] prepared an apparatus to electrospin acrylic fibers with diameters in the range of 500 nm–1.1 μm. Although the electrospinning process has shown promising potential and has existed for several decades in the literature, the process has remained essentially unchanged and its understanding is still limited [12].

In the 1990s, a great interest in electrospinning research was generated when Doshi and Reneker [13] reintroduced this technique to make submicron fibers. Polyacrylonitrile (PAN) and copolymers of PAN have been widely studied for almost a century for commercial/technological exploitations. PAN may be cross-linked, but also may exist without crosslinking. Crosslinking of PAN will impart some of its important physical properties, such as insolubility and resistance to swelling in common organic solvents. Recently, considerable efforts have been devoted to its processing and fiber forming technologies.

Among the various precursors for producing carbon nanofibers (CNFs), PAN is the most commonly used polymer, mainly due to its high carbon yield (up to 56%), flexibility for tailoring the structure of the final CNFs products and the ease of obtaining stabilized products due to the formation of a ladder structure via nitrile polymerization [14–19]. Also, PAN is a well-known polymer with good stability and mechanical properties, has been widely used in producing CNFs as these have attracted much recent attention due to their excellent characteristics, such as spinnability, environmentally benign nature and commercial viability.

The chemistry of PAN is of particular interest because of its use as a precursor in the formation of CNFs for different applications, including porous structured CNFs of high surface area for electronics and energy storage applications as well as graphite

* Corresponding author. Tel./fax: +20 552304987.
E-mail addresses: ashali@zu.edu.eg, hassanien65@yahoo.com (A.A. Ali).

http://dx.doi.org/10.1016/j.elstat.2014.09.003
0304-3886/

reinforcement filaments for organic materials in high strength and high stiffness composites. The recent review by Inagaki et al. [20] describes the chemistry and applications of CNFs, restricted mainly to the research on scientific and technological developments in Japan.

Barhate and Ramakrishna [21] published a review on nanofibers as a filtering media for tiny materials. Li and Xia [22] discussed about the trends in nanofibers with emphasis on electrospinning techniques to produce nanofibers.

PAN nanofibres and carbon nanotube (CNT) reinforced PAN nanofibres were successfully electrospun [23]. Ali [24–28] published a series of publications studying the characteristics of the electrospun PAN/*N*,*N*-dimethylformamide (DMF) polymer solution using both wet and dry collectors, before and after heat treatment, with and without nano reinforcements. In his work optimization of the process for PAN nanofibers has been introduced without using any statistical analysis such as response surface methodology (RSM).

RSM has been used successfully for process optimization in many studies such as polymer electrospinning and polymer hydrogels [29–31]. Process optimization of nanofibers based layers has been investigated by RSM in order to predict the domain of the parameters where the smallest fiber diameter can be achieved. A quantitative relationship between electrospinning parameters and the responses (mean diameter and standard deviation) was established and then the final multi-layers structure of nanofibers and nanoparticles has been achieved for a controlled and robust process [32–34].

In this work RSM has been used to optimize the electrospun PAN by studying the effect of five major processing parameters on electrospun PAN fiber diameter and its standard deviation.

The selected five major parameters are:

1. Berry's number: dimensionless parameter measures the degree of molecular chain entanglement and it is equal to the product of PAN concentration by PAN/DMF intrinsic viscosity. Berry's number covers polymer molecular weight, polymer concentration and polymer/solvent solubility parameter. So, it can be used as a more generalized bench mark scale to measure molecular conformation including PAN molecular weight, concentration and solvent type. Equation of Berry's number is given below:

$$\text{Berry's number} = \text{intrinsic viscosity} \times \text{concentration} \quad (1)$$

where; intrinsic viscosity is the ratio of specific viscosity to concentration at infinite dilution.

2. Charge density: measures the amount of applied voltage (kV) divided by the linear distance (cm) between the spinneret and the collector center.
3. Spinneret diameter: measures the inside diameter of the metal needle of flatten end (mm).
4. Spinning angle: measures the inclination angle with the vertical axis connecting between the spinneret center and the collector center (degree).
5. Collector size: measures the collector area (cm^2).

Experimental

Preparation of polymer solution

PAN of 150,000 g/mol molecular weight from Aldrich, catalog no. (181315) was used with 4–12% weight concentration in DMF to form a polymer solution after hot stirring for 3 h at 60 °C to ensure a complete solubility. The intrinsic viscosity has been measured by using Ostwald viscometer and its value for the used PAN/DMF polymer solution found to be equal one (exact value = 1.0044).

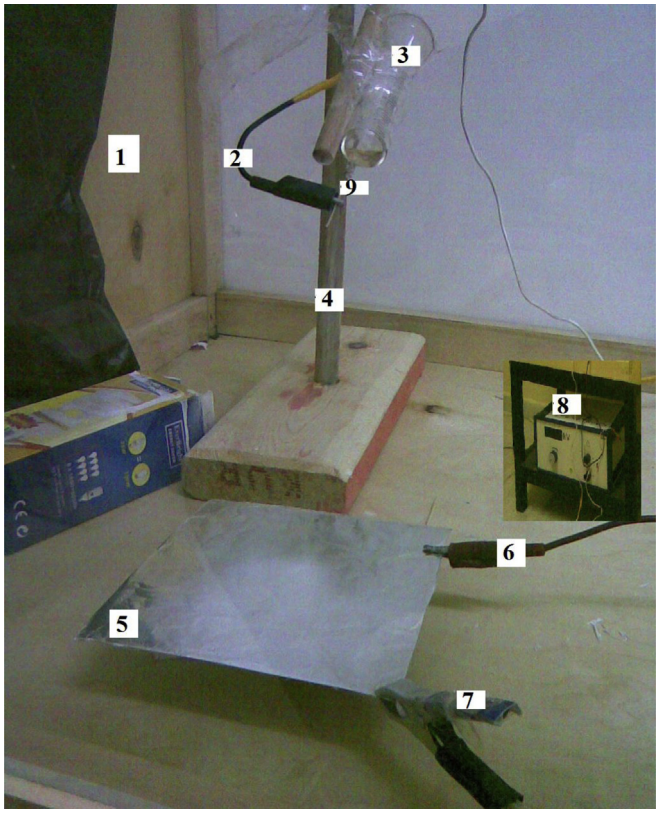

Fig. 1. Electrospinning set-up: 1. Control box – 2. Positive charged electrode – 3. Glass syringe – 4. Wooden stand – 5. Metal collector – 6. Grounded counter electrode – 7. Collector adjusted hand – 8. High voltage source – 9. Metal needle.

Electrospinning set-up

The electrospinning setup was assembled in our lab as shown in Fig. 1.The spinning solution was placed in 10 ml glass syringe with a metal needle of different diameters. Metal needle was connected to a high voltage power supply generates DC voltage up to 25 kV. A flat metal plate with aluminum foil was placed below and serving as a grounded counter electrode. The voltage between the electrode and the counter electrode was controlled by the high voltage power supply. A stable drop of the solution was suspended at the tip of the capillary before the power was supplied. Morphology of the collected PAN fibers were studied by using scanning electron microscopy (SEM) after drying under vacuum at room temperature for 24 h.

Design of experiments

The accuracy and effectiveness of an experimental program depends on careful planning and execution of the experimental

Table 1
Coded and actual values of the input parameters.

Input parameters	Symbol	Levels				
		−2	−1	0	1	2
Spinning angle (θ)	X_1	15	30	45	60	75
Charge density (kV/cm)	X_2	1	1.3	1.6	1.9	2.2
Berry's number	X_3	4	6	8	10	12
Spinneret diameter (mm)	X_4	0.5	0.7	0.9	1.1	1.3
Collector area (cm^2)	X_5	25	100	175	250	325

Table 2
Experimental design matrix and experimental results.

Exp. no.	Input process parameter					Exp. results	
	Spinning angle (θ)	Charge density (kV/cm)	Berry's no.	Spinneret dia. (mm)	Collector size (cm^2)	Average fiber diameter (nm)	STDEV (nm)
1	30	1.3	6	0.7	250	196	39
2	60	1.3	6	0.7	100	220	42
3	30	1.9	6	0.7	100	285	38
4	60	1.9	6	0.7	250	264	38
5	30	1.3	10	0.7	100	210	57
6	60	1.3	10	0.7	250	226	47
7	30	1.9	10	0.7	250	329	110
8	60	1.9	10	0.7	100	325	68
9	30	1.3	6	1.1	100	214	39
10	60	1.3	6	1.1	250	241	32
11	30	1.9	6	1.1	250	249	49
12	60	1.9	6	1.1	100	256	40
13	30	1.3	10	1.1	250	346	83
14	60	1.3	10	1.1	100	414	98
15	30	1.9	10	1.1	100	321	67
16	60	1.9	10	1.1	250	434	120
17	15	1.6	8	0.9	175	284	45
18	75	1.6	8	0.9	175	257	50
19	45	1	8	0.9	175	223	50
20	45	2.2	8	0.9	175	268	50
21	45	1.6	4	0.9	175	104	27
22	45	1.6	12	0.9	175	364	94
23	45	1.6	8	0.5	175	297	50
24	45	1.6	8	1.3	175	306	58
25	45	1.6	8	0.9	25	340	69
26	45	1.6	8	0.9	325	297	32
27	45	1.6	8	0.9	175	282	30
28	45	1.6	8	0.9	175	282	26
29	45	1.6	8	0.9	175	282	27
30	45	1.6	8	0.9	175	282	29
31	45	1.6	8	0.9	175	282	26
32	45	1.6	8	0.9	175	282	30

procedures with a view to achieving a minimum average fiber diameter. The effect of Berry's number (Five adjusted concentrations have been used to study the effect of Berry's number calculated from Equation (1)), charge density, spinning angle, spinneret diameter and collector area were investigated. In this work, experiments were carried out according to a central composite second order rotatable design which has been chosen from the software options after Montgomery [33] recommendation for similar number of experimental variables based on response surface methodology (RSM). Design of experiments (DOE) and features

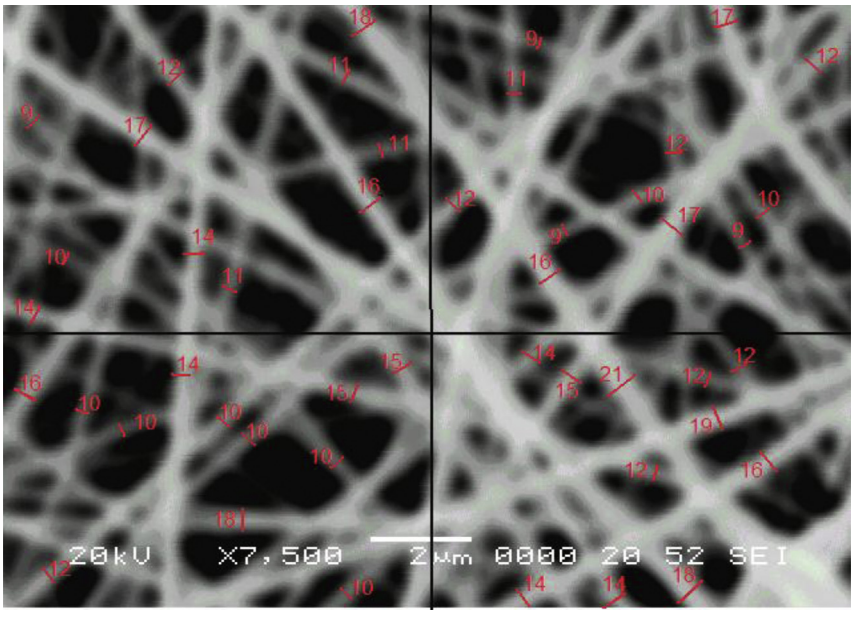

Fig. 2. Measurement of average nanofiber diameter.

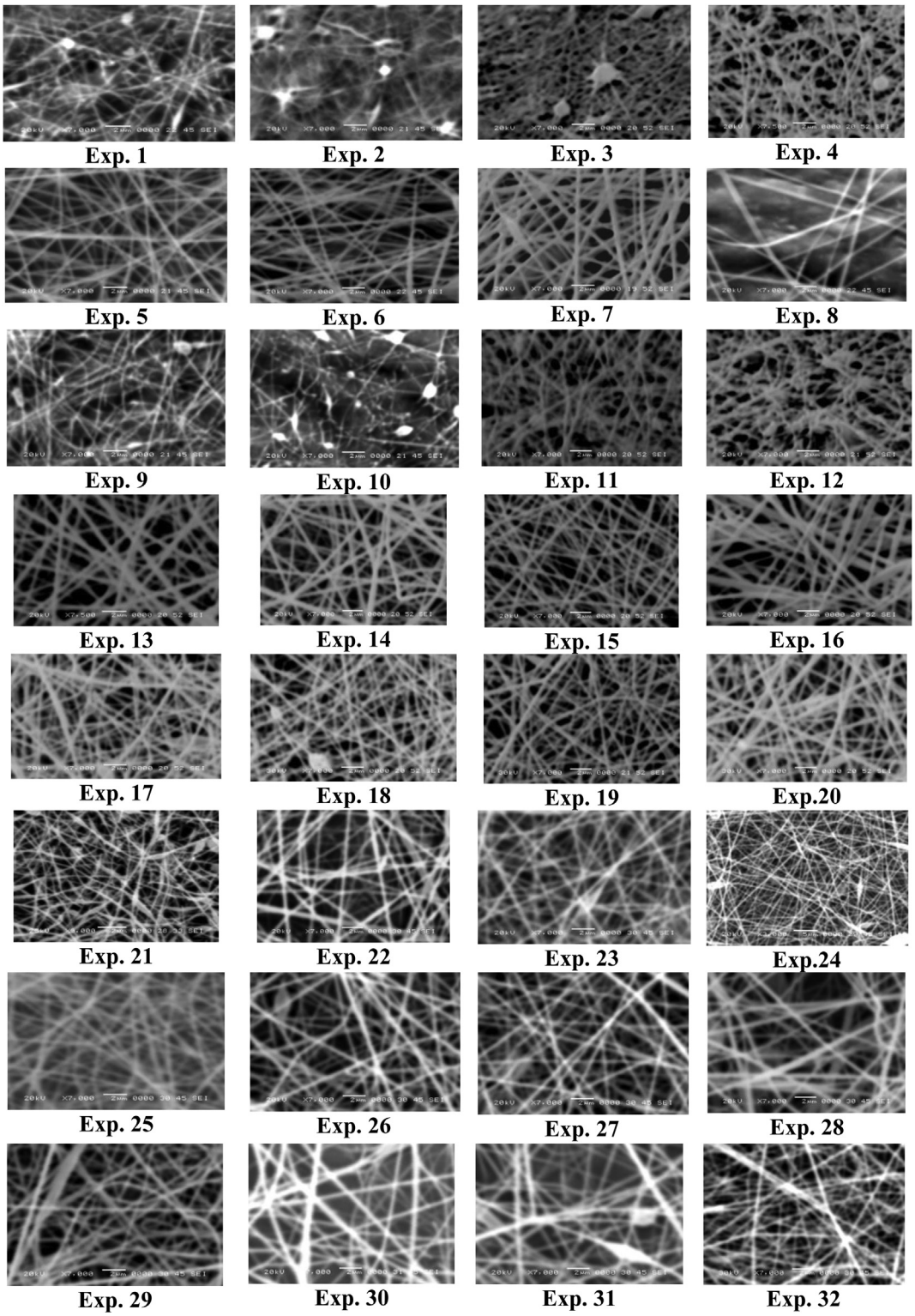

Fig. 3. Morphology of nanofibers at experimental design matrix (electrospinning parameters of each Exp. no. are shown in Table 2).

of Design Expert-6 software were utilized as well to determine the coefficients of mathematical modeling based on the response surface regression model. These developed models are very helpful to predict average fiber diameter and standard deviation of fiber diameter for the proposed values of input variables and to select an optimum combination of input variables for the average fiber diameter and standard deviation of electrospun fiber diameters. Design Expert-6 software also produces ANOVA tables to test lack of fit of the RSM-based models, and offers the “graphic option” to obtain a response surface plot for the selected parametric ranges of the developed response surfaces. The electrospinning parameters are arranged in five levels as shown in Table 1. The experimental

design was based on 5 factors, 5 levels each, and 6 replicates at central points. The design of experiment counted 32 runs and for every sample the response, fiber diameter, has been recorded from SEM micrographs as previously mentioned. The results of the recorded mean diameter and the relative standard deviation for every set of experiments are shown in Table 2.

3. Measurement and characterization

Morphology

The morphology of electrospun PAN fibers was investigated by scanning electron microscopy (JEOL JSM-5600LV) after being gold-coated. Each of SEM pictures was divided into four equal regions as shown in Fig. 2 then same amount of measured fibers were taken from each quarter. The diameters were measured precisely by correlating the number of the points used by the software to the given measured distance from the SEM in each picture under a suitable magnification.

Results and discussion

Electro-spun PAN fiber morphology

Fig. 3 shows the morphology of electrospun PAN nanofibers have been collected from input parameters shown in Table 2. Spindle-like beads was collected at Berry's no. = 6 and charge density 1.3 kV/cm as shown in Fig. 3 (Exp. 1, 2, 9, and 10) as charge density increases to 1.9 kV/cm for same Berry's number a spindle-like beads formation decreases and more uniform fibers were collected as shown in Fig. 3 (Exp. 3 & 4). As Berry's numbers increases from 6 to 10 and up to 12 for same charge density beads were disappeared and more uniform fibers were collected. As shown in Fig. 3 (Exp. 5, 6, 7, 8, and 12) and Fig. 3 (Exp. 6) as Berry's number = 10, charge density = 1.3 kV/cm, PAN average fiber diameters of 210 ± 47 nm were collected. As shown in Fig. 3 (Exp. 7 and 8) as Berry's number = 10, charge density = 1.9 kV/cm, PAN average fiber diameters of 320 ± 110 nm and 352 ± 68 nm were collected. The average values and standard deviations of fiber diameters were taken for statistical analysis.

The mathematical modeling for nanofibers based layers

The relationship between the five factors (Berry's number, charge density, spinning angle, spinning diameter and collector area) and the response was approximated by a second-order polynomial model:

$$y = \beta_0 + \sum_{i=1}^{k} \beta_i X_i + \sum_{i=1}^{k} \beta_{ij} X^2 + \sum_{i} \sum_{j} \beta_{ij} X_i X_j + \varepsilon \qquad (2)$$

The coefficient β_0 is the free term, the coefficients β_i are the linear terms, the coefficients β_{ij} are the interaction terms, and the coefficients β_{ii} are the quadratic terms. Using the results shown in Table 2, the full form of the derived models could be extracted. The adequacies of the models were checked by using the analysis of variance ANOVA. Through this technique, the F- ratio for each term in the developed model was determined to know the significant and non-significant terms. Furthermore, the lake of fit of each model was determined to measure the deviation of the response from the fitted surface. Design Expert software was used to analyze the experimental data of the response parameters. In addition, Design Expert software produces ANOVA Tables to test the lack of fit of the RSM-based models.

Table 3
Actual mathematical model of the average fiber diameter.

		y = average fiber diameter (nm)
		+280.57955
	$*X_1$	+0.845833
	$*X_2$	+21.37500
	$*X_3$	+47.79167
	$*X_4$	+17.12500
	$*X_5$	−3.04167
$*X_2$	$*X_1$	−0.81250
$*X_3$	$*X_1$	+11.43750
$*X_4$	$*X_1$	+10.81250
$*X_5$	$*X_1$	−10.43750
$*X_3$	$*X_2$	+3.56250
$*X_4$	$*X_2$	−20.81250
$*X_5$	$*X_2$	+6.93750
$*X_4$	$*X_3$	+25.18750
$*X_5$	$*X_3$	+3.93750
$*X_5$	$*X_4$	+7.31250
	$*X_1^2$	−1.45455
	$*X_2^2$	−7.70455
	$*X_3^2$	−5.57955
	$*X_4^2$	+6.29545
	$*X_5^2$	+10.54545

Effect of electrospinning parameters on average fiber diameter

Based on Equation (2), the effect of input parameters, shown in Table 1, on the average fiber diameter has been evaluated by computing the values of various constants using Design Expert software and the relevant experimental results from Table 2. The mathematical model of the average fiber diameter can be expressed as shown in Table 3.

where y is average fiber diameter in (nm), X_1, X_2, X_3, X_4, and X_5 are the coded values of spinning angle (θ in degree), charge density (kV/cm), Berry's number, spinneret diameter (mm) and collector size (cm^2) respectively. From Table 3 it can be noticed that; the model F-value of 7.15 which implies the average fiber diameter model is significant. There is only a 0.09% chance that a "Model F-Value" this large could occur due to noise. In this case X_2, X_3, X_4, X_2X_4 and X_3X_4 are significant model terms. Values of "Prob > F" less than 0.05 indicate model terms are significant. Values greater than 0.1 indicate the model terms are not significant. The "Pred R-Squared" of 90.70% is in reasonable agreement with the "Adj R-Squared" of 79.87%. "Adeq Precision" measures the signal to noise

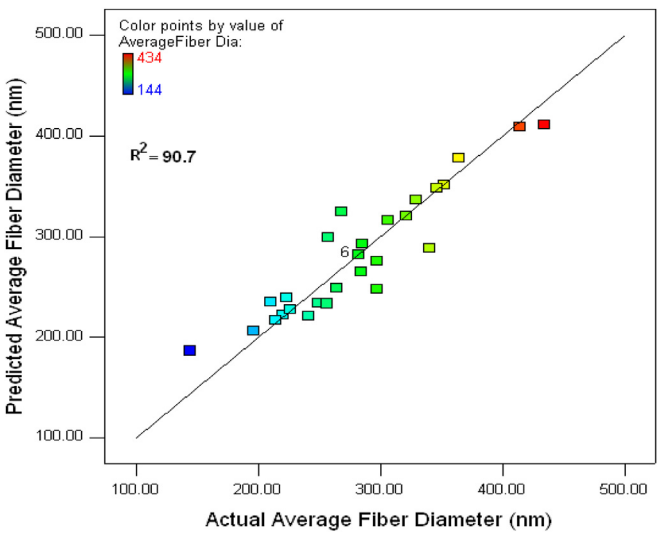

Fig. 4. Predicted vs. measured values of average fiber diameter.

Table 4
Actual mathematical model of STDEV.

		y = STDEV (nm)
		+27.85227
	$^*X_1$	+0.54167
	$^*X_2$	+3.87500
	$^*X_3$	+18.79167
	$^*X_4$	+4.37500
	$^*X_5$	−0.20833
$^*X_2$	$^*X_1$	+0.062500
$^*X_3$	$^*X_1$	+1.81250
$^*X_4$	$^*X_1$	+6.31250
$^*X_5$	$^*X_1$	−5.68750
$^*X_3$	$^*X_2$	+4.18750
$^*X_4$	$^*X_2$	−2.81250
$^*X_5$	$^*X_2$	+8.68750
$^*X_4$	$^*X_3$	+5.18750
$^*X_5$	$^*X_3$	+4.43750
$^*X_5$	$^*X_4$	+0.68750
	$^*X_1^2$	+5.02273
	$^*X_2^2$	+5.64773
	$^*X_3^2$	+9.27273
	$^*X_4^2$	+6.64773
	$^*X_5^2$	+5.77273

ratio. The model ratio is 11.207 indicates an adequate signal. This model has been used to navigate the design space. The previous mathematical model Table 3, the experimental and the predicted data are plotted in Fig. 4.This scatter diagram and ANOVA Table 6 clearly show that; the predictions made by the average fiber diameter mathematical model Table 3 are in a good agreement with the experimental data.

Effect of electrospinning parameters on STDEV

Based on Equation (2), the effect of input parameters (Table 1) on the STDEV have been evaluated by computing the values of various constants using Design Expert software and the relevant experimental results from Table 2. The mathematical model of the STDEV can be expressed as shown in Table 4.

where y is fiber STDV in (nm) and X_1, X_2, X_3, X_4, and X_5 are the coded values of spinning angle (θ in degree), charge density (kV/cm), Berry's number, spinneret diameter (mm) and collector size (cm^2) respectively. From Table 6, it can be noticed that the model F-value of 6.76 which implies the STDEV model is significant. There is only a 0.12% chance that a "Model *F*-Value" this large could occur due to noise. In this case X_3, X_2X_5, X_1^2, X_2^2, X_3^2, X_4^2 and X_5^2 are significant model terms. Values of "Prob > *F*" less than 0.05 indicate model terms are significant. Values greater than 0.1 indicate the model terms are not significant. The "Lack of Fit *F*-value" of 66.38 implies the Lack of Fit is significant. There is only a 0.01% chance that a "Lack of Fit *F*-value" this large could occur due to noise. The "Pred *R*-Squared" of 92.5% is in reasonable agreement with the "Adj *R*-Squared" of 79.5%. "Adeq Precision" measures the signal to noise ratio. The model ratio is 8.930 indicates an adequate signal. This model can be used to navigate the design space. The previous mathematical model Table 4, the experimental and the predicted

Table 5
ANOVA for RS average fiber diameter.

Source	Sum of squares	df	Mean square	*F* value	*P*-value Prob > *F*
Model	1.074×10^5	20	5370.82	7.15	0.0009
X_1	1717.04	1	1717.04	2.29	0.1588
X_2	10965.38	1	10965.3	14.60	0.0028
X_3	54817.04	1	54817.0	72.97	<0.0001
X_4	7038.38	1	7038.38	9.37	0.0108
X_5	222.04	1	222.04	0.30	0.5975
X_1X_2	10.56	1	10.56	0.014	0.9078
X_1X_3	2093.06	1	2093.06	2.79	0.1233
X_1X_4	1870.56	1	1870.56	2.49	0.1429
X_1X_5	1743.06	1	1743.06	2.32	0.1559
X_2X_3	203.06	1	203.06	0.27	0.6134
X_2X_4	6930.56	1	6930.56	9.23	0.0113
X_2X_5	770.06	1	770.06	1.03	0.3331
X_3X_4	10150.56	1	10150.5	13.51	0.0037
X_3X_5	248.06	1	248.06	0.33	0.5771
X_4X_5	855.56	1	855.56	1.14	0.3088
X_1^2	62.06	1	62.06	0.083	0.7791
X_2^2	1741.23	1	1741.23	2.32	0.1561
X_3^2	913.19	1	913.19	1.22	0.2938
X_4^2	1162.56	1	1162.56	1.55	0.2394
X_5^2	3262.06	1	3262.06	4.34	0.0613
Residual	8263.77	11	751.25		
Lack of fit	8263.77	6	1377.30		
Pure error	0.000	5	0.000		
Cor total	1.157×10	31			

Table 6
ANOVA for RS (STDEV).

Source	Sum of squares	df	Mean square	*F* value	*P*-value Prob > *F*
Model	17843.68	20	892.18	6.76	0.0012
X_1	7.04	1	7.04	0.053	0.8216
X_2	360.38	1	360.38	2.73	0.1267
X_3	8475.04	1	8475.04	64.21	<0.0001
X_4	459.38	1	459.38	3.48	0.0890
X_5	1.04	1	1.04	7.892×10^{-3}	0.9308
X_1X_2	0.063	1	0.063	4.735×10^{-4}	0.9830
X_1X_3	52.56	1	52.56	0.40	0.5409
X_1X_4	637.56	1	637.56	4.83	0.0503
X_1X_5	517.56	1	517.56	3.92	0.0732
X_2X_3	280.56	1	280.56	2.13	0.1728
X_2X_4	126.56	1	126.56	0.96	0.3485
X_2X_5	1207.56	1	1207.56	9.15	0.0116
X_3X_4	430.56	1	430.56	3.26	0.0983
X_3X_5	315.06	1	315.06	2.39	0.1506
X_4X_5	7.56	1	7.56	0.057	0.8152
X_1^2	740.02	1	740.02	5.61	0.0373
X_2^2	935.64	1	935.64	7.09	0.0221
X_3^2	2522.18	1	2522.18	19.11	0.0011
X_4^2	1296.31	1	1296.31	9.82	0.0095
X_5^2	977.52	1	977.52	7.41	0.0199
Residual	1451.82	11	131.98		
Lack of fit	1433.82	6	238.97	66.38	0.0001
Pure error	18.00	5	3.60		
Cor total	19295.50	31			

Where DF is the Degree of freedom.

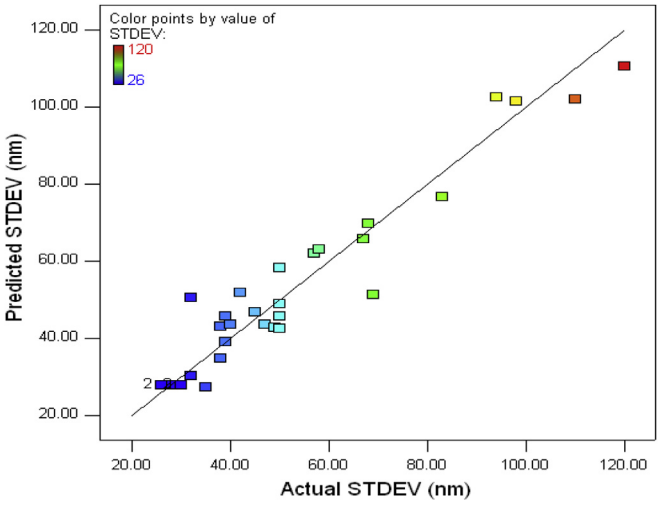

Fig. 5. Predicted vs. measured values of STDV.

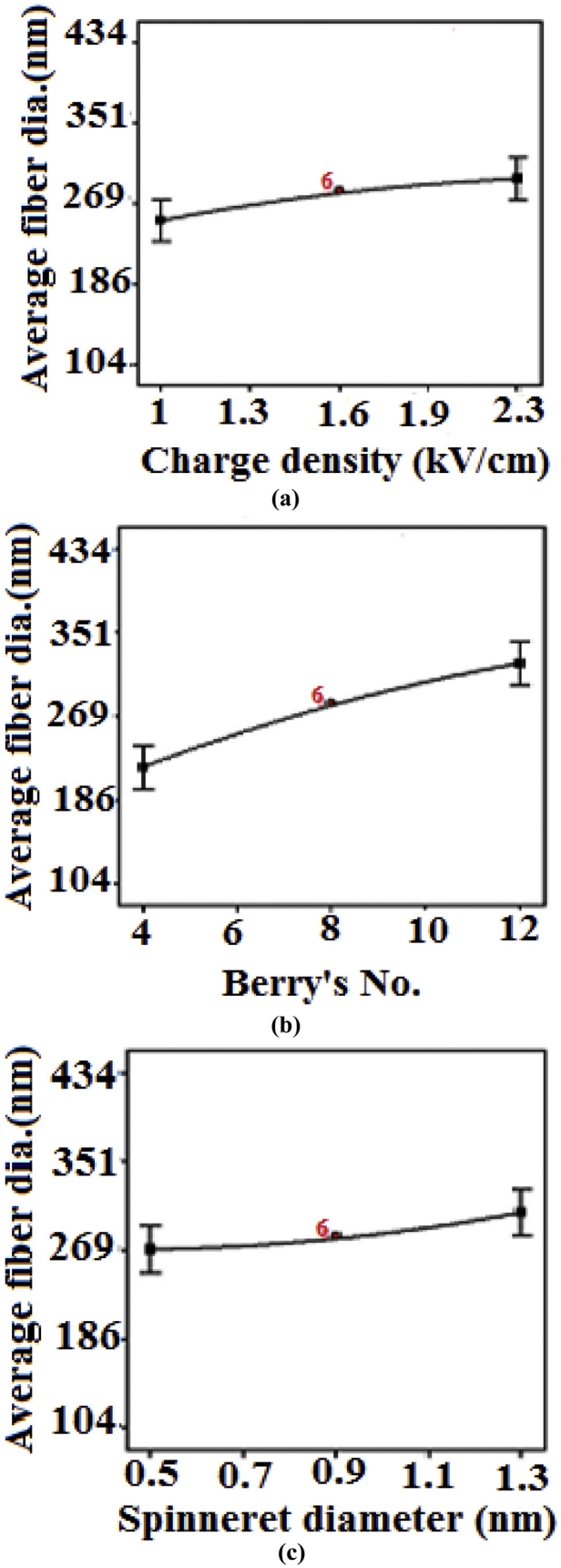

Fig. 6. Main effect plots of (a) charge density, (b) Berry's number and (c) spinneret diameter on average fiber diameter.

data are plotted in Fig. 5.This scatter diagram and ANOVA clearly show that, the predictions made by the STDEV mathematical model (Table 4) are in a good agreement with the experimental data (Table 5).

Main effect plots and interaction plot of factors on average fiber diameter

As shown in Fig. 6a–c the effect of charge density, Berry's number and spinneret diameter on the collected PAN average fiber diameter by using RSM indicates a more uniformity for electrospun PAN fibers at 1.6 kV/cm charge density, Berry's number of 8 with 0.9 mm spinneret diameter.

As shown in Fig. 6a the effect of charge density on the collected PAN average fiber diameter by using RSM indicates more uniformity for electrospun PAN fibers at1.6 kV/cm charge density. As shown in Fig. 6b the effect of Berry's number on the collected PAN average fiber diameter by using RSM indicates more uniformity for electrospun PAN fibers at 8 Berry's number. Also As shown in Fig. 6c the effect of spinneret diameter on the collected PAN average fiber diameter by using RSM indicates a more uniformity for electrospun PAN fibers at 0.9 mm spinneret diameter.

Conclusions

The effect of the specified five major electrospinning processing parameters (Berry's number, charge density, spinneret diameter, spinning angle and collector size) on electrospun PAN fiber by using RSM can be summarized in the following points:

1. The RSM mathematical model can be used to predict the average fiber diameter and its standard deviation as well as to optimize the assigned electrospinning parameters within the specified regions.
2. The RSM mathematical model concluded that; charge density, Berry's number, and spinneret diameter have a significant impact and play an important role on average fiber diameter and its standard deviation. On the other hand, collector area and spinning angle have a non-significant impact on the electrospun PAN average fiber diameter.
3. A minimum PAN average fiber diameter of 280 ± 28 nm was reported at 1.6 kV/cm charge density, 8 Berry's number and 0.9 mm spinneret diameter based on the RSM mathematical model.

References

[1] J. Zeleny, Instability of electrified liquid surfaces, Phys. Rev. 10 (1917) 1–6.
[2] A. Formhals, Processing and Apparatus for Preparing Artificial Threads, US Patent 2,077,373, 1934.
[3] A. Formhals, Method of Producing Artificial Fiber, US Patent 2,158,415, 1939.
[4] A. Formhals, Production of Artificial Fibers Forming Liquids, US Patent 2,323,025, 1943.
[5] A. Formhals, Method and Apparatus for Spinning, US Patent 2,349,950, 1944.
[6] H.L. Simmons, U.S. Patent 3,280,229, 1966.
[7] G.I. Taylor, Disintegration of water drops in an electric field, in: Proceedings of the Royal Society, Series A, Mathematical, Physical & Engineering Sciences, London, vol. 280 (1382), 1964, pp. 383–397.
[8] G.I. Taylor, A.D. McEwan, Stability of a horizontal fluid interface in a vertical electric field, J. Fluid Mech. 22 (1965) 1–15.
[9] J.R. Melcher, G.I. Taylor, Electrohydrodynamics: a review of the role of interfacial shear stresses, Ann. Rev. Fluid Mech. 1 (1969) 111–146.
[10] G.I. Taylor, Electrically driven jets, in: Proceedings of the Royal Society of London, Series A, Mathematical, Physical & Engineering Sciences, London, vol. 313, 1969, pp. 453–475.
[11] P.K. Baumgarten, J. Colloid Interface Sci. 36 (1971) 7.
[12] Z.M. Haung, Y.Z. Zhang, M. Kotaki, S. Ramakrishna, Compos. Sci. Technol. 63 (2003) 2223.
[13] J. Doshi, D.H. Reneker, Electrospinning process and applications of electrospun fibers, J. Electrost. 3 (1995) 151–160.

[14] Y. Liang, L. Ji, B. Guo, Z. Lin, Y.F. Yao, Y. Li, M. Alcoutlabi, Y. Qiu, X. Zhang, Preparation and electrochemical characterization of ionic conducting lithium lanthanum titanate oxide/polyacrylonitrile submicron composite fiber-based lithium-ion battery separators, J. Power Sources 196 (2011) 436–441.
[15] C.E. Schildknecht, Vinyl and Related Polymers; Their Preparations, Properties and Applications in Rubbers, Plastics and in Medical and Industrial Arts, Wiley-Interscience, New York, 1952, p. 3878.
[16] K.E. Perepelkin, N.V. Klyuchnikova, N.A. Kulikova, Experimental evaluation of man-made fibre brittleness, Fibre Chem. 21 (1989) 145–148.
[17] M.S.A. Rahaman, A.F. Ismail, A. Mustafa, A review of heat treatment on polyacrylonitrile fiber, Polym. Degrad. Stab. 92 (2007) 1421–1432.
[18] A.D. Litmanovich, N.A. Plate, Alkaline hydrolysis of polyacrylonitrile; on the reaction mechanism, Macromol. Chem. Phys. 201 (2000) 2176–2180.
[19] S.K. Nataraj, K.S. Yang, T.M. Aminabhavi, Polyacrylonitrile-based nanofibers – a state-of-the-art review, Prog. Polym. Sci. 37 (3) (2012) 487–513.
[20] M. Inagaki, K. Kaneko, T. Nishizawa, Nanocarbons – recent research in Japan, Carbon 42 (2004) 1401–1417.
[21] R.S. Barhate, S. Ramakrishna, Review nanofibrous filtering media: filtration problems and solutions from tiny materials, J. Membr. Sci. 296 (2007) 1–8.
[22] D. Li, Y. Xia, Electrospinning of nanofibers: reinventing the wheel? Adv. Mater. 16 (2004) 1151–1170.
[23] Mohammad Kazemi Pilehrood, Pirjo Heikkilä, Ali Harlin, Preparation of carbon nanotube embedded in PAN nanofiber composites by electrospinning process, AUTEX Res. J. 12 (1) (March 2012). ©AUTEX.
[24] A.A. Ali, Wet electrospun nanofibers, in: Al-Azhar Engineering Eights International Conference, Egypt, December 24–27, 2004.
[25] A.A. Ali, M. El-Hamid, Electrospinning optimization for precursor carbon nanofiber, Compos. A 37 (2006) 1681–1687.
[26] A.A. Ali, Self-assembled ultra-fine carbon coils by wet electrospinning, Mater. Lett. 60 (2006) 2858–2862.
[27] A.A. Ali, G.C. Rutledge, Hot-pressed electrospun PAN nanofibers: an idea for flexible carbon mat, J. Mater. Process. Technol. 209 (2009) 4617–4620.
[28] A.A. Ali, Al-Asmari A. Kh, Wet-electrospun CuNP/carbon nano fiber composites: potential application for surface mounted component, Appl. Nanosci. 2 (2012) 55–61.
[29] S. Sukigara, M. Gandhi, J. Ayutsede, M. Micklus, F. Ko, Regeneration of Bombyx mori silk by electrospinning, part 2. Process optimization and empirical modeling using response surface methodology, Polymer 45 (2004) 3701.
[30] R. Wächter, A. Cordery, Response surface methodology modeling of diamond like carbon film deposition, Carbon 37 (1999) 1529.
[31] C.C. Hung, H.C. Lin, H.C. Shih, Response surface methodology applied to silicon trench etching in $Cl_2/HBr/O_2$ using transformer coupled plasma technique, Solid-State Electron. 46 (2002) 791.
[32] Martina Roso, Alessandra Lorenzetti, Stefano Besco, Manuel Monti, Guido Berti, Michele Modesti, Application of empirical modeling in multi-layers membrane manufacturing, Comput. Chem. Eng. 35 (2011) 2248–2256.
[33] D.C. Montgomery, Design and Analysis of Experiments, Wiley, New York, 2001.
[34] S.R. Ghabrial, S.J. Ebeid, S.M. Serag, M.M. Ayad, A mathematical modeling for electrochemical turning, in: PEDAC 5th International Conference, 1992, pp. 449–459.